East European Journal of Physics. 3. 103-114 (2025)
DOI:10.26565/2312-4334-2025-3-10 ISSN 2312-4334

WAVE PROPAGATION IN ANISOTROPIC MAGNETICALLY QUANTIZED ION PLASMA WITH TRAPPED ELECTRON AND POSITRON

Balaram Pradhan[a], Apul Narayan Dev[b]*, Manoj Kumar Deka[c]
[a]Center for Data science, Siksha 'O' Anusandhan (Deemed to be University), Khandagiri, Bhubneswar 751030, Odisha, India
[b]Department of Mathematics, Siksha 'O' Anusandhan (Deemed to be University), Khandagiri, Bhubneswar 751030, Odisha, India
[c]Department of Radiography and Imaging Technology, Srimanta Sankaradeva University of Health Sciences, Guwahati 781032, India
*Corresponding Author E-mail: apulnarayan@gmail.com; apulnarayandev@soa.ac.in
Received June 8, 2025; revised July 6, 2025; in final form August 8, 2025; accepted August 18, 2025

This study examines the effects of magnetically quantized degenerate trapped electrons and positrons on small-amplitude ion acoustic shock waves (IAShWs) in a pair ion plasma using the Zakharov-Kuznetsov Burger (ZKB) equation. It focuses on how factors like magnetic quantization, degenerate temperature, normalized negative ions, electrons, positrons, anisotropic pressure, and other relevant physical parameters from an astrophysical plasma environment influence the propagation of IAShWs, particularly in the nonlinear regime. This research explores that there exist two distinct wave propagation modes—subsonic and supersonic which shows few distinct characteristics in different physical plasma environment of astrophysical origin. The results could aid in understanding the nonlinear dynamics and wave propagation characteristics in superdense plasmas found in white dwarfs and neutron stars, where the effects of trapped electrons and positrons, as well as ionic pressure anisotropy, are significant which is yet to be explored in detail.
Keywords: *Magnetized plasma; Subsonic and supersonic modes; Reductive perturbation method (RPT); Degenerate trapped electrons and positrons; ZKB equation; Phase plane analysis*
PACS: 52.35. Fp, 52.35. Mw, 52.27. Ep, 52.25. Xz, 52.27.Cm, 52.35.Ra

1. INTRODUCTION

The field of degenerate dense plasmas is attracting more attention, resulting in a significant amount of research activity. As scientists explore this area further, new insights and discoveries are being made [1-3]. These plasmas are found in highly dense astrophysical environments, including white dwarf stars [4, 5, 6] and neutron stars [7, 8, 9], among other locations. In these extreme settings, the physical conditions allow for the formation and stability of such plasmas. Several researchers have explored nonlinear waves in degenerate plasma systems (DPS) that include both positive and negative ions, as well as electrons and positrons [10-14]. Their studies focus on understanding the complex interactions within these plasmas, which can lead to fascinating phenomena such as solitons and wave packets. Jahangir R. et al. [15] investigate the nonlinear dynamics of IAShWs in a magnetized plasma with trapped electrons. Their study examines how degenerate electrons and temperature influence the amplitude and width of shock waves. Nonlinear localized wave excitation in non-equilibrium plasmas with particle flow have been investigated in [16-19] kinetic approximation with trapped electrons. Kaur R. et al. [20] explore the characteristics of IAShWs and the structure of oscillatory shock waves in ion beam plasma, which contains positive ions and trapped electrons within a quantizing magnetic field. They found that the amplitude of the oscillatory shock waves increases as the quantizing parameter rises. Iqbal M. J. et al. [21] examine the solitary wave structures in a plasma made up of degenerate electrons and positrons in the presence of a quantizing magnetic field. El-Borie M. A. et al. [22] study the properties of ion-acoustic waves in a magnetized plasma made up of positively and negatively charged fluid ions and trapped electrons. They analyze how various plasma parameters, including electron degenerate temperature, electron trapping effects, and viscosity, influence the profile of small yet finite amplitude solitary and shock waves. Shah H. A. et al. [23] examine the impact of trapping in a degenerate quantum plasma that includes nondegenerate ions and degenerate electrons. They found solitary wave structures when the electrons are fully degenerate, while in weakly nondegenerate plasma, both rarefactive and compressive solitary wave structures appear with changes in temperature. In a multi-ion plasma composed of positive and negative ions and trapped electrons, the nonlinear propagation of ion acoustic solitary waves (IASWs) and IAShWs are investigated by El-Monier S. Y. et al [24]. They noticed the effect of different plasma parameters on IASWs and IAShWs profile. IAShWs in a pair of ion magnetized plasma is investigated by Yeashna T. et al [25]. They observed both compressive and rarefactive shock potentials and the effect of oblique angle and kinematic viscosity on that profile. Zedan N. A. et al. [26] examined IASWs in a collisionless magnetized plasma that includes a degenerate pair of ions and trapped electrons within a quantizing magnetic field. In a theoretical investigation on dust ion acoustic waves in a degenerate electron-positron-ion (EPI) plasma the influence of viscosity on shock wave profile is studied by Halder et. al. [27]. Hussian S. et al. [28] investigated electron-ion degenerate plasma considering trapping effects and Landau quantization. They concluded that increasing kinematic viscosity and obliqueness strengthens the shock. In a theoretical investigation of shock waves in a degenerate magnetized plasma, Asaduzzaman M. et al. [29] analysed

Cite as: B. Pradhan, A.N. Dev, M.K. Deka, East Eur. J. Phys. 3, 103 (2025), https://doi.org/10.26565/2312-4334-2025-3-10

how variations in kinematic viscosity, obliqueness, and number density significantly affect the characteristics of amplitude and steepness. Small amplitude IASWs are studied by Deka M. K. & Dev A. N. [30] on a magnetically quantized degenerate plasma consisting trapped electrons and positrons.

In a strong magnetic field, plasma exhibits anisotropic pressure characterized by distinct parallel and perpendicular components. This occurs under adiabatic conditions, influenced by rapid changes in plasma density as waves propagate. These variations in density can significantly affect the plasma's behavior, leading to unique wave dynamics and interactions that are crucial for understanding plasma stability and confinement in various astrophysical and laboratory settings. Irfan M. et al [31] studied characteristics of the ion-acoustic waves (IAWs) in the presence of ionic pressure anisotropy and electron trapping effects in a dense magnetoplasma consisting of degenerate relativistic trapped electrons and they reported that ionic pressure anisotropy has a significant effect on the amplitude of solitary potential both in relativistic and non-relativistic cases. Jahan. S. et al [32] studied the IAShWs in a degenerate magnetoplasma consisting of degenerate electrons, inertial nonrelativistic partially charged heavy and light ions. In their observation, it was concluded that the number density of non-relativistic heavy and light ions enhances the amplitude of IAShWs and the steepness of the shock profile is decreased with kinematic viscosity. In a rigorous investigation on degenerate EPI plasma, Rahman A. U. et al [33] studied the effect of key plasma parameters such as ion-electron temperature ratio, positron-electron density ratio and degeneracy parameter on solitary wave structure. The effect of anisotropic pressure and viscosity on the propagation of shock waves in a degenerate quantum magneto plasma is studied by Deka M. K. et al [34]. The aim of this manuscript is to investigate the propagation of IAShWs in magnetoplasma which consists of degenerate electrons, positrons, and ions, with the effects of viscosity. As far as we know, no one has yet made an effort to explore the nonlinear structures of IAShWs in the current context. This lack of investigation highlights a significant gap in our understanding, which could potentially hinder the progress in this field. The manuscript is arranged as follows. The basic equations are normalized by using normalized parameter in Sec. 2. In Sec. 3 the ZKB equation is derived from normalised equation. The influence of physical parameter on the profile of shock waves are discussed in Sec. 4. In Sec. 5 the phrase portrait analysis is performed by using Galian transformation. Finally, the brief conclusion is provided in Sec. 6.

2. MATHEMATICAL MODEL FOR DYNAMIC EQUATIONS

Let us consider a collision-less magneto plasma consisting of positive and negative ions along with trapped electrons and positrons is considered in the current investigation. The presence of external magnetic field ($B = B_o\hat{x} \neq 0$, where $\hat{x}$ is the unit vector along the x-axes) causes the inertial ions to exhibit pressure anisotropy.
The occupation number density of degenerate electrons and positrons can be expressed as [20,23,24,27,30]

$$N_j = \frac{p_{F_j}^2 \eta_j}{2\pi^2\hbar^3}\sqrt{\frac{m_j}{2}}\sum_{l=0}^{\infty}\int_0^{\infty}\frac{\varepsilon^{-1/2}}{1+\exp\left(\left(\varepsilon-U\right)/T\right)}d\varepsilon \tag{1}$$

Here, μ is the chemical potential, $\eta = \hbar\omega_{ce}/\varepsilon_{Fe}$ is representing the effect of the quantizing magnetic field appears though the modified electron Fermi energy $\varepsilon_{Fe} = \left(\hbar^2/2m_e\right)\left(3\pi^2 n_{e0}\right)^{2/3}$ and $n_{e0} = \left(p_{Fe}^3/3\pi^2\hbar^3\right)$. Again, the momentum of the fermi surface is denoted by p_{Fe} , the degenerate temperature is $T = \left(\pi T_e/2\sqrt{2}\,\varepsilon_{Fe}\right)$ and the potential is $\Psi = e\psi/\varepsilon_{Fe}$. By adopting the standard procedures for replacing the summation by integration of Eq. (1) for electron density, we obtain

$$N_e = N_{e0}\left\{\frac{3}{2}H\left(1+\Psi\right)^{\frac{1}{2}} + \left(1+\Psi-H\right)^{\frac{3}{2}} - \frac{HT^2}{2}\left(1+\Psi\right)^{-\frac{3}{2}} + T^2\left(1+\Psi-H\right)^{-\frac{1}{2}}\right\}$$

Which on expanding becomes

$$\left.\begin{aligned} n_e = &\frac{\eta}{2}\left(3-T^2\right) + \left(1-\eta\right)^{\frac{3}{2}} + T^2\left(1-\eta\right)^{-\frac{1}{2}} + \frac{3\psi}{2}\left\{\frac{\eta}{2}\left(1+T^2\right) + \left(1-\eta\right)^{\frac{1}{2}} - \frac{T^2}{3}\left(1-\eta\right)^{-\frac{3}{2}}\right\} \\ &+\frac{3\psi^2}{8}\left\{-\frac{\eta}{2}\left(1+5T^2\right) + \left(1-\eta\right)^{-\frac{1}{2}} + T^2\left(1-\eta\right)^{-\frac{5}{2}}\right\} \end{aligned}\right\} \tag{2}$$

Similarly, we obtain the expression for positron density as

$$N_p = N_{p0}\left\{\begin{aligned} &\frac{3\,\eta}{2}\mu_p^{-\frac{2}{3}}\left(1-\psi\mu_p^{-\frac{2}{3}}\right)^{1/2} - \frac{\eta T^2}{2}\mu_p^{-2}\left(1-\psi\mu_p^{-\frac{2}{3}}\right)^{-3/2} + \left(1-\psi\mu_p^{-\frac{2}{3}} - \eta\mu_p^{-\frac{2}{3}}\right)^{3/2} \\ &+\mu_p^{-\frac{4}{3}}T^2\left(1-\psi\mu_p^{-\frac{2}{3}} - \eta\mu_p^{-\frac{2}{3}}\right)^{-1/2} \end{aligned}\right\}$$

On expanding, the above equations become

$$\left.\begin{aligned} n_p &= \frac{\eta\mu_p^{-\frac{2}{3}}}{2}\left(3-\mu_p^{-\frac{4}{3}}T^2\right)+\left(1-\mu_p^{-\frac{2}{3}}\eta\right)^{\frac{3}{2}}+\mu_p^{-\frac{4}{3}}T^2\left(1-\mu_p^{-\frac{2}{3}}\eta\right)^{-\frac{1}{2}} \\ &+\frac{3\psi}{2}\left\{-\frac{\eta\mu_p^{-\frac{4}{3}}}{2}\left(1+\mu_p^{-\frac{4}{3}}T^2\right)-\mu_p^{-\frac{2}{3}}\left(1-\mu_p^{-\frac{2}{3}}\eta\right)^{\frac{1}{2}}+\frac{\mu_p^{-2}T^2}{3}\left(1-\mu_p^{-\frac{2}{3}}\eta\right)^{-\frac{3}{2}}\right\} \\ &+\frac{3\psi^2}{8}\left\{-\frac{\eta\mu_p^{-2}}{2}\left(1+5\mu_p^{-\frac{4}{3}}T^2\right)+\mu_p^{-\frac{4}{3}}\left(1-\mu_p^{-\frac{2}{3}}\eta\right)^{-\frac{1}{2}}+\mu_p^{-\frac{8}{3}}T^2\left(1-\mu_p^{-\frac{2}{3}}\eta\right)^{-\frac{5}{2}}\right\} \end{aligned}\right\} \tag{3}$$

The unnormalized govern equations for such plasma are read as

$$\frac{\partial N_\pm}{\partial T}+\nabla\left(N_\pm V_\pm\right)=0 \tag{4}$$

$$\left(\frac{\partial}{\partial T}+\vec{V}_\pm\nabla\right)\vec{V}_\pm=\frac{Z_\pm e}{m_\pm}\left(\mp\vec{\nabla}\Psi+\vec{V}_\pm\times B\right)-\frac{1}{m_\pm n_\pm}\nabla P_\pm+\delta_\pm\vec{\nabla}^2\vec{V}_\pm+\left(\delta_\pm+\rho_\pm\right)\vec{\nabla}\left(\vec{\nabla}\vec{V}_\pm\right) \tag{5}$$

$$\nabla^2\Psi=4\pi e\left(N_e+Z_-N_--Z_+N_+-N_p\right) \tag{6}$$

In the above plasma system, $N_\pm$ is ion fluid density (+ sign represents for positive ion and – sign represents for negative ion) which is normalized by equilibrium unperturbed number density $N_{\pm0}$, $V_\pm$ is the positive and negative ion fluid velocity which is normalized by ion acoustic speed $C_s\left(v_\pm=V_\pm\times C_s\right)$, the corresponding space variable is normalized by Debye length $\left(\lambda_D=\sqrt{K_BT_e/4\pi N_e e^2}\right)$ and the time variable is by plasma frequence $\left(\omega_{pi}=\sqrt{4\pi N_{+0}e^2/m_+}\right)$. The external magnetic field $\left(\Omega_\pm=Z_\pm eB\lambda_D/m_\pm C_s\right)$, kinematic viscosity $\left(\delta_\pm=\delta_\pm^{/}/C_s\lambda_D\right)$ and bulk viscosity $\left(\rho_\pm=\rho_\pm^{/}/C_s\lambda_D\right)$ is normalized by λ_D and C_s. The other plasma parameter such as potential function is normalized by $\Psi=e\psi/\varepsilon_{Fe}$, the pressure term along the parallel direction is $P_{\pm ll}=P_{\pm ll0}\left(N_\pm/N_{\pm0}\right)^3$ and along the perpendicular direction is $P_{\pm\perp}=P_{\pm\perp}\left(N_\pm/N_{\pm0}\right)$. Thus, at equilibrium the charge neutrality condition of our plasma model can be written as $\mu_m+\mu_e=1+\mu_p$.

After normalization, the basic set of equations for positive and negative ions are expressed as

$$\frac{\partial n_+}{\partial t}+\frac{\partial}{\partial x}\left(n_+u_{+x}\right)+\frac{\partial}{\partial y}\left(n_+u_{+y}\right)+\frac{\partial}{\partial Z}\left(n_+u_{+z}\right)=0 \tag{7}$$

$$\left.\begin{aligned} &\frac{\partial u_{+x}}{\partial t}+\left(u_{+x}\frac{\partial}{\partial x}+u_{+y}\frac{\partial}{\partial y}+u_{+z}\frac{\partial}{\partial z}\right)u_{+x}=-Z_+\frac{\partial\phi}{\partial x}+\left(\vec{u}_{+x}\times\Omega_+\right)-\bar{P}_{+\|}n_+\frac{\partial n_+}{\partial x} \\ &+\delta_{+\|}^{/}\left(\frac{\partial^2}{\partial x^2}+\frac{\partial^2}{\partial y^2}+\frac{\partial^2}{\partial z^2}\right)\left(u_{+x}\right)+\left(\delta_{+\|}^{/}+\rho_{+\|}^{/}\right)\left(\frac{\partial^2u_{+x}}{\partial x^2}+\frac{\partial^2u_{+y}}{\partial x\partial y}+\frac{\partial^2u_{+z}}{\partial x\partial z}\right) \end{aligned}\right\} \tag{8}$$

$$\left.\begin{aligned} &\frac{\partial u_{+y}}{\partial t}+\left(u_{+x}\frac{\partial}{\partial x}+u_{+y}\frac{\partial}{\partial y}+u_{+z}\frac{\partial}{\partial z}\right)u_{+y}=-Z_+\frac{\partial\phi}{\partial y}+\left(\vec{u}_{+y}\times\Omega_+\right)-\bar{P}_{+\perp}\frac{1}{n_+}\frac{\partial n_+}{\partial y} \\ &+\delta_{+\perp}^{/}\left(\frac{\partial^2}{\partial x^2}+\frac{\partial^2}{\partial y^2}+\frac{\partial^2}{\partial z^2}\right)\left(u_{+y}\right)+\left(\delta_{+\perp}^{/}+\rho_{+\perp}^{/}\right)\left(\frac{\partial^2u_{+x}}{\partial y\partial x}+\frac{\partial^2u_{+y}}{\partial y^2}+\frac{\partial^2u_{+z}}{\partial y\partial z}\right) \end{aligned}\right\} \tag{9}$$

$$\left.\begin{aligned} &\frac{\partial u_{+z}}{\partial z}+\left(u_{+x}\frac{\partial}{\partial x}+u_{+y}\frac{\partial}{\partial y}+u_{+z}\frac{\partial}{\partial z}\right)u_{+z}=-Z_+\frac{\partial\phi}{\partial z}+\left(\vec{u}_{+z}\times\Omega_+\right)-\bar{P}_{+\perp}\frac{1}{n_+}\frac{\partial n_+}{\partial z} \\ &+\delta_{+\perp}^{/}\left(\frac{\partial^2}{\partial x^2}+\frac{\partial^2}{\partial y^2}+\frac{\partial^2}{\partial z^2}\right)\left(u_{+z}\right)+\left(\delta_{+\perp}^{/}+\rho_{+\perp}^{/}\right)\left(\frac{\partial^2u_{+x}}{\partial z\partial x}+\frac{\partial^2u_{+y}}{\partial z\partial y}+\frac{\partial^2u_{+z}}{\partial z^2}\right) \end{aligned}\right\} \tag{10}$$

$$\frac{\partial n_-}{\partial t}+\frac{\partial}{\partial x}\left(n_-u_{-x}\right)+\frac{\partial}{\partial y}\left(n_-u_{-y}\right)+\frac{\partial}{\partial z}\left(n_-u_{-z}\right)=0 \tag{11}$$

$$\left.\begin{aligned}&\frac{\partial u_{-x}}{\partial t}+\left(u_{-x}\frac{\partial}{\partial x}+u_{-y}\frac{\partial}{\partial y}+u_{-z}\frac{\partial}{\partial z}\right)u_{-x}=\gamma Z_-\frac{\partial\phi}{\partial x}-\left(\vec{u}_{-x}\times\Omega_-\right)-\gamma\bar{P}_{-\parallel}n_-\frac{\partial n_-}{\partial x}\\&+\delta'_{-\parallel}\left(\frac{\partial^2}{\partial x^2}+\frac{\partial^2}{\partial y^2}+\frac{\partial^2}{\partial z^2}\right)\left(u_{-x}\right)+\left(\delta'_{-\parallel}+\rho'_{-\parallel}\right)\left(\frac{\partial^2u_{-x}}{\partial x^2}+\frac{\partial^2u_{-y}}{\partial x\partial y}+\frac{\partial^2u_{-z}}{\partial x\partial z}\right)\end{aligned}\right\} \tag{12}$$

$$\left.\begin{aligned}&\frac{\partial u_{-y}}{\partial t}+\left(u_{-x}\frac{\partial}{\partial x}+u_{-y}\frac{\partial}{\partial y}+u_{-z}\frac{\partial}{\partial z}\right)u_{-y}=\gamma Z_-\frac{\partial\phi}{\partial y}-\left(\vec{V}_{-z}\times\Omega_-\right)-\gamma\bar{P}_{-\perp}\frac{1}{n_-}\frac{\partial n_-}{\partial y}\\&+\delta'_{-\perp}\left(\frac{\partial^2}{\partial x^2}+\frac{\partial^2}{\partial y^2}+\frac{\partial^2}{\partial z^2}\right)\left(u_{-y}\right)+\left(\delta'_{-\perp}+\rho'_{-\perp}\right)\left(\frac{\partial^2u_{-x}}{\partial y\partial x}+\frac{\partial^2u_{-y}}{\partial y^2}+\frac{\partial^2u_{-z}}{\partial y\partial z}\right)\end{aligned}\right\} \tag{13}$$

$$\left.\begin{aligned}&\frac{\partial u_{-z}}{\partial t}+\left(u_{-x}\frac{\partial}{\partial x}+u_{-y}\frac{\partial}{\partial y}+u_{-z}\frac{\partial}{\partial z}\right)u_{-z}=\gamma Z_-\frac{\partial\phi}{\partial z}-\left(\vec{u}_{-z}\times\Omega_-\right)-\gamma\bar{P}_{-\perp}\frac{1}{n_-}\frac{\partial n_-}{\partial z}\\&+\delta'_{-\perp}\left(\frac{\partial^2}{\partial x^2}+\frac{\partial^2}{\partial y^2}+\frac{\partial^2}{\partial z^2}\right)\left(u_{-z}\right)+\left(\delta'_{-\perp}+\rho'_{-\perp}\right)\left(\frac{\partial^2u_{-x}}{\partial z\partial x}+\frac{\partial^2u_{-y}}{\partial z\partial y}+\frac{\partial^2u_{-z}}{\partial z^2}\right)\end{aligned}\right\} \tag{14}$$

$$\frac{\partial^2\psi}{\partial x^2}+\frac{\partial^2\psi}{\partial y^2}+\frac{\partial^2\psi}{\partial z^2}=\left(n_e\mu_e+Z_-n_-\mu_m-Z_+n_+-n_P\mu_p\right) \tag{15}$$

Where, $\mu_e\left(n_{e0}/n_{+0}\right)$ is electron to positive ion density ratio, $\mu_m\left(n_{-0}/n_{+0}\right)$ is negative to positive ion density ratio and $\mu_p\left(n_{p0}/n_{+0}\right)$ is the positron to positive ion density ratio.

3. DERIVATION OF TKDVB EQUATION

To study the nonlinear properties of ion-acoustic shock waves (IAShWs) in a collisionless pair of ion plasma (PIP), we adopt the method of reductive perturbation (MRP). According to this method for small amplitude waves the following stretched variables are used to derived ZKB equation [14,15]

$$\left.\begin{aligned}&\xi=\varepsilon^{1/2}\left(X-\lambda T\right),\ \eta=\varepsilon^{1/2}Y\ ,\ \zeta=\varepsilon^{1/2}Z,\ \ \tau=\varepsilon^{3/2}T\\&\delta'_{\pm}=\varepsilon^{1/2}\delta_{\pm}\ \ and\ \ \rho'_{\pm}=\varepsilon^{1/2}\rho_{\pm}\end{aligned}\right\} \tag{16}$$

Where λ shows the linearized phase velocity of the IAShWs and its perturbed amplitude is measuring by the real small dimensionless parameter $\varepsilon(<<1)$.

The dependent physical variables of the above equation such as density (n), velocity (u) and potential function (ψ) are expanded asymptotically as a power series near the equilibrium state as follows:

$$\left.\begin{aligned}&n_{\pm}=1+\sum_{j=1}^{\infty}\varepsilon^j n_{\pm}^{(1)}, &&u_{\pm x}=\sum_{j=1}^{\infty}\varepsilon^j u_{\pm x}^{(1)}\\&u_{\pm y,z}=\sum_{j=1}^{\infty}\sum_{k=0}\varepsilon^{1+\frac{j}{2}}u_{\pm y,z}^{(1+k)}, &&\psi=\sum_{j=1}^{\infty}\varepsilon^j\psi^{(j)}\end{aligned}\right\} \tag{17}$$

Now, substituting the above perturbation scheme (Eqs. 16 & 17) in the set of normalized equations (7)-(15) and collecting the coefficients of lower order of $\varepsilon\ \left(\sim\varepsilon^{3/2}\right)$ as follows:

$$\left.\begin{aligned}&N_+^{(1)}=\frac{-Z_+}{\left(\bar{P}_{+\parallel}-\lambda^2\right)}\psi^{(1)},N_-^{(1)}=\frac{\gamma Z_-}{\left(\gamma\bar{P}_{-\parallel}-\lambda^2\right)}\psi^{(1)},N_e^{(1)}=\frac{\psi^{(1)}}{\alpha_1},\ N_p^{(1)}=\frac{\psi^{(1)}}{\Upsilon_1}\\&V_{+x}^{(1)}=\lambda N_+^{(1)},\ V_{+y}^{(1)}=\frac{1}{\Omega_+}\left(Z_+\frac{\partial\psi^{(1)}}{\partial\eta}+\bar{P}_{+\perp}\frac{\partial N_+^{(1)}}{\partial\eta}\right),\ V_{+z}^{(1)}=\frac{1}{\Omega_+}\left(Z_+\frac{\partial\psi^{(1)}}{\partial\zeta}+\bar{P}_{+\perp}\frac{\partial N_+^{(1)}}{\partial\zeta}\right)\\&V_{-x}^{(1)}=\lambda N_-^{(1)},\ V_{-y}^{(1)}=\frac{\gamma}{\Omega_-}\left(Z_-\frac{\partial\psi^{(1)}}{\partial\eta}-\bar{P}_{-\perp}\frac{\partial N_-^{(1)}}{\partial\eta}\right),\ V_{-z}^{(1)}=\frac{\gamma}{\Omega_-}\left(Z_-\frac{\partial\psi^{(1)}}{\partial\zeta}-\bar{P}_{-\perp}\frac{\partial N_-^{(1)}}{\partial\zeta}\right)\end{aligned}\right\} \tag{18}$$

Where, $\alpha_1 = \frac{3}{2}\left\{\frac{\eta}{2}\left(1+T^2\right)+\left(1-\eta\right)^{\frac{1}{2}}-\frac{T^2}{3}\left(1-\eta\right)^{-\frac{3}{2}}\right\}$ and $\Upsilon_1 = \frac{\eta\delta^{-\frac{2}{3}}}{2}\left(3-\delta^{-\frac{4}{3}}T^2\right)+\left(1-\delta^{-\frac{2}{3}}\eta\right)^{\frac{3}{2}}+\delta^{-\frac{4}{3}}T^2\left(1-\delta^{-\frac{2}{3}}\eta\right)^{-\frac{1}{2}}$

Proceeding in same way from lowest order of poissons equation we obtain the expression for phase velocity as:

$$\lambda^2 = \frac{q \pm \sqrt{q^2-4pr}}{2p}. \tag{19}$$

Here,

$p = \left(\Upsilon_1\mu_e - \alpha_1\mu_P\right)$;

$q = \left(\alpha_1\Upsilon_1\left(Z_+^2+\gamma\mu_m Z_-^2\right)+\left(\Upsilon_1\mu_e-\alpha_1\mu_P\right)\left(\overline{P}_{+\parallel}+\gamma\overline{P}_{-\parallel}\right)\right)$;

$r = \left(\gamma\overline{P}_{+\parallel}\overline{P}_{-\parallel}\left(\Upsilon_1\mu_e-\alpha_1\mu_P\right)+\alpha_1\Upsilon_1\left(Z_+^2\gamma\overline{P}_{-\parallel}+\gamma\mu_m\overline{P}_{+\parallel}Z_-^2\right)\right)$

Similarly, continuing the same process for next higher order of ε gives rise the expression for the second order perturbation terms. After a few algebraic operations with the help of Eq. (18), we obtain the ZKB equation as:

$$\left.\begin{aligned}&\frac{\partial\psi^{(1)}}{\partial\tau}+B\psi^{(1)}\frac{\partial\psi^{(1)}}{\partial\xi}+C\frac{\partial^3\psi^{(1)}}{\partial\xi^3}-D_2\left(\frac{\partial^2\psi^{(1)}}{\partial\xi^2}+\frac{\partial^2\psi^{(1)}}{\partial\eta^2}+\frac{\partial^2\psi^{(1)}}{\partial\zeta^2}\right)\\&-D_1\frac{\partial^2\psi^{(1)}}{\partial\xi^2}+F\frac{\partial}{\partial\xi}\left(\frac{\partial^2\psi^{(1)}}{\partial\eta^2}+\frac{\partial^2\psi^{(1)}}{\partial\zeta^2}\right)=0\end{aligned}\right\} \tag{20}$$

Where the nonlinearity of the system is $B = b/a$, the dispersion term $C=-1/a$, the dissipation coefficient due to bulk viscosity and kinematic viscosity are respectively $D_1 = d_1/a$, $D_2 = d_2/a$ and $F = f/a$ is the transverse term.

While $a = \left(-\frac{2\lambda Z_+^2}{\left(\overline{P}_{+\parallel}-\lambda^2\right)^2}-\frac{2\lambda\gamma\mu_m Z_-^2}{\left(\gamma\overline{P}_{-\parallel}-\lambda^2\right)^2}\right)$,

$$b = \left(\alpha_2\mu_e-\Upsilon_2\mu_P+Z_+^3\frac{3\lambda^2+\overline{P}_{-\parallel}}{\left(\overline{P}_{-\parallel}-\lambda^2\right)^3}-\mu_m Z_-^3\frac{3\lambda^2+\gamma\overline{P}_{-\parallel}}{\left(\gamma\overline{P}_{-\parallel}-\lambda^2\right)^3}\right)$$

$$\alpha_2 = \frac{3}{8}\left\{-\frac{\eta}{2}\left(1+5T^2\right)+\left(1-\eta\right)^{-\frac{1}{2}}+T^2\left(1-\eta\right)^{-\frac{5}{2}}\right\}$$

$$\Upsilon_2 = \frac{3}{2}\left\{-\frac{\eta\delta^{-\frac{4}{3}}}{2}\left(1+\delta^{-\frac{4}{3}}T^2\right)-\delta^{-\frac{2}{3}}\left(1-\delta^{-\frac{2}{3}}\eta\right)^{\frac{1}{2}}+\frac{\delta^{-2}T^2}{3}\left(1-\delta^{-\frac{2}{3}}\eta\right)^{-\frac{3}{2}}\right\}$$

$$d_1 = \left(Z_+^2\frac{\left(\delta_{+\parallel}+\rho_{+\parallel}\right)}{\left(\overline{P}_{+\parallel}-\lambda^2\right)^2}+\lambda Z_-^2\frac{\left(\delta_{-\parallel}+\rho_{-\parallel}\right)}{\left(\gamma\overline{P}_{-\parallel}-\lambda^2\right)^2}\right)$$

$$d_2 = \left(\frac{Z_+^2\delta_{+\parallel}}{\left(\overline{P}_{+\parallel}-\lambda^2\right)^2}-\frac{\lambda\mu_m Z_-^2\delta_{-\parallel}}{\left(\gamma\overline{P}_{-\parallel}-\lambda^2\right)^2}\right)$$

$$f = \left(-\frac{\lambda^2}{\Omega_+^2}\frac{Z_+^2}{\left(\overline{P}_{+\parallel}-\lambda^2\right)}-\frac{\lambda^2}{\Omega_-^2}\frac{\gamma\mu_m Z_-^2}{\left(\gamma\overline{P}_{-\parallel}-\lambda^2\right)}+\frac{\lambda^2}{\Omega_+^2}\frac{\overline{P}_{+\perp}Z_+^2}{\left(\overline{P}_{+\parallel}-\lambda^2\right)^2}+\frac{\lambda^2}{\Omega_-^2}\frac{\gamma^2\mu_m Z_-^2\overline{P}_{-\perp}}{\left(\gamma\overline{P}_{-\parallel}-\lambda^2\right)^2}-1\right)$$

4. RESULTS AND DISCUSSIONS

In this section, we investigate the effects of variations of different plasma parameters on the characteristics of IAShWs governed by Eq. (20). For that purpose, we have considered the range of some typical physical parameters in dense astrophysical environments (neutron stars and white dwarfs) in which degenerate EPI is important. The well-defined parameters are considered as the equilibrium density $\eta_{io} = 10^{26} - 10^{29} cm^{-3}$, $n_{eo(p0)} = 10^{28} - 10^{30} cm^{-3}$ [9,14,15,23], $B_o = 10^9 - 10^{12} G$ [15,20,23] and the Fermi temperature for those parameters in the range of $3.6277\times10^7 K$ [20,30].

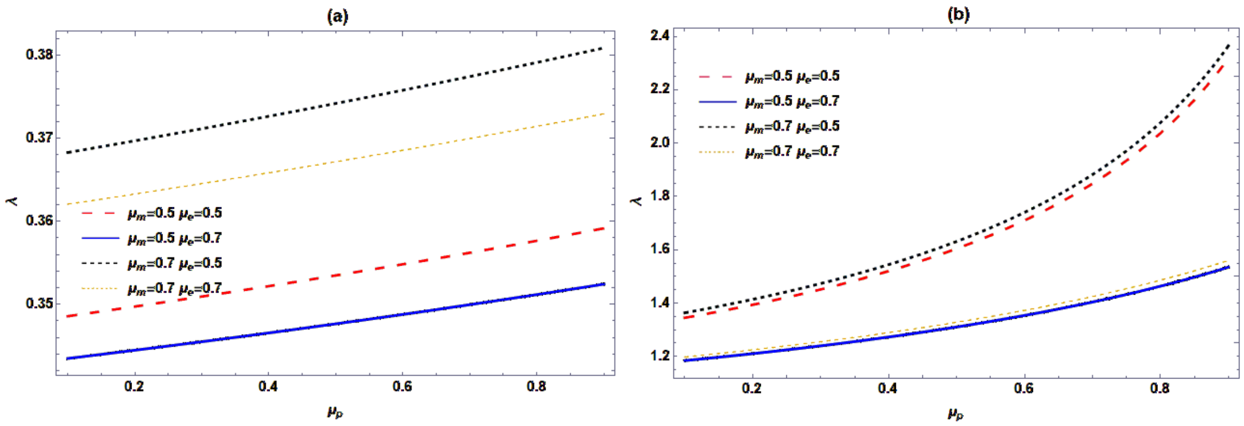

Figure 1 The variation of normalized phase speed λ represented by Eq. (19) is depicted against μ_p for (a) subsonic $(\lambda < 1)$ and (b) supersonic $(\lambda > 1)$ situations with several values of μ_m and μ_e

We have investigated the impact of critical plasma parameters on phase speed, as our goal is to analyze the characteristics of ion acoustic modes in the plasma system under consideration. The plasma model being analysed can have both fast and slow modes. Fig.1 presents the normalized phase velocity (λ) of the wave as a function of the ratio of positron-to-positive ion equilibrium density (μ_p). This data is displayed for various values of the electron-to-positive ion equilibrium density ratio (μ_e) and the negative-to-positive ion equilibrium density ratio (μ_m), covering both (a) subsonic and (b) supersonic mode. The Fig. 1(a) reveals that λ decreases as the μ_e increases. In contrast, it rises with higher ratios of μ_p and μ_m. In both figures, the phase velocity is lowest when the electron density μ_e is higher than the electron μ_m density. This happens because, as positron density increases, electron density may also increase due to matter-antimatter annihilation. As a result, the concentration of heavier negative ions increases, which reduces the phase velocity. On the other hand, if electron density decreases while negative ion density increases with positron density, the total positive ion density becomes higher, causing the phase velocity to increase. This situation corresponds to the black dashed curve in Fig. 1(a) and Fig. 1(b).

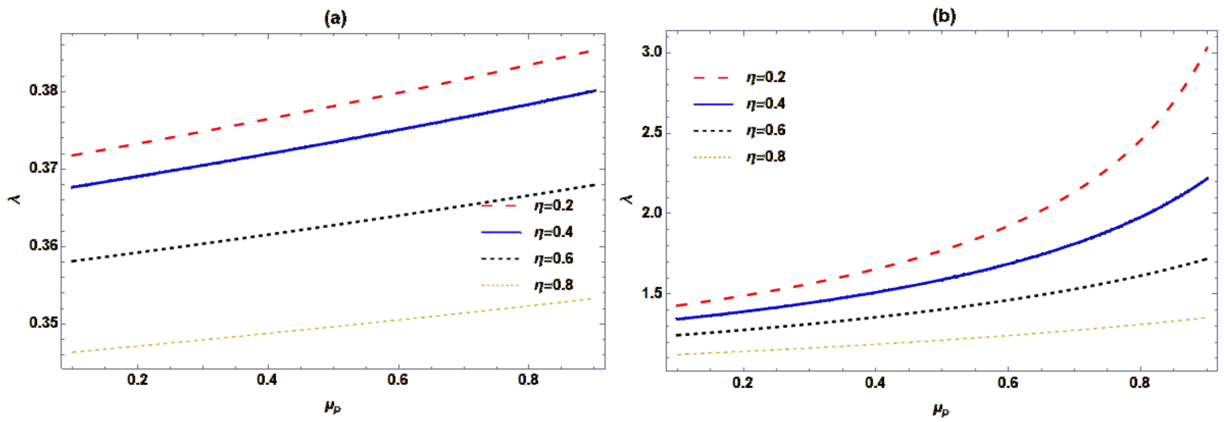

Figure 2. The variation of normalized phase speed λ represented by Eq. (19) is depicted against μ_p for (a) subsonic $(\lambda < 1)$ and (b) supersonic $(\lambda > 1)$ situations with several values of η .

The Fig. 2 shows the variation of normalized phase velocity (λ) by changing the quantization parameter (η) for two ion acoustic modes (a) subsonic and (b) supersonic. From both Fig. 2, it is observed that the λ decreases with increasing η [26]. This is because as the quantization parameter increase which eventually means an increase in the strength of magnetic field, more and more electron will be trapped and hence phase velocity will be reduced.

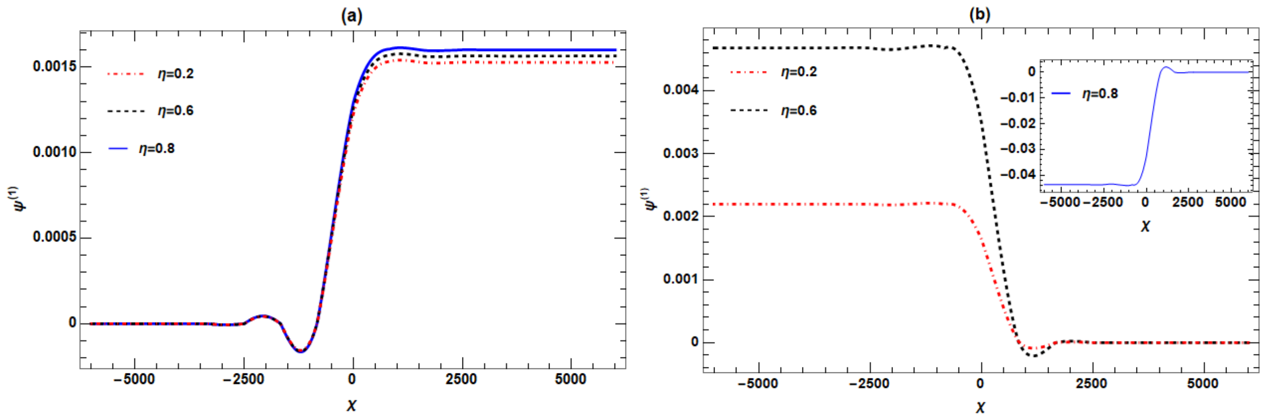

Figure 3. Showing the profile $\psi^{(1)}$ of IAShWs that represented by Eq. (20) against χ with combination of different normalized density values $\mu_{m,}$ μ_e and μ_p for $(a)\lambda<1$ and $(b)\lambda>1$, while the values of other parameter is considered as $\delta_+=0.5,$ $\delta_-=0.5,$ $\Omega_+=0.6, \Omega_+=0.16,$ $l=0.3,$ $p_{+\|}=0.5, p_{+\perp}=0.2, p_{-\|}=0.3$ & $p_{-\perp}=0.2$

Fig. 3 demonstrates the graphical representation of normalized potential function $\psi^{(1)}$ (as a function of spatial distance χ) with different values of quantizing magnetic field effect appears through the parameter (η) and temperature (T) for (a) subsonic and (b) supersonic modes respectively. From Fig. 3(a), it is noticed that when the normalized phase speed is in subsonic mode, the increase in η increases the steepness of shock wave without affecting the amplitude of the waves. However, from Fig. 3(b), it is observed that as η increases the amplitude and steepness of shock wave increase, but after a particular value of $\eta \geq 0.8$ the polarity of shock potential changes from positive to negative. The quantizing parameters influence both the phase velocity of the shock wave and the nonlinearity within the plasma system. Next, we investigate the influence of obliqueness parameter l on the profile of IAShWs potential profile $\psi^{(1)}$ for both (a) subsonic and (b) supersonic normalized phase velocity λ . Fig. 4(a) shows that the amplitude of IAShWs is strongly dependent on l and it is observed that as l increases, the amplitude as well as steepness of shock profile decreases rapidly. However, when the phase speed is in supersonic range the increase in l initially increases the amplitude and steepness, after a certain value it reduced the shock profile (Fig. 4(b)) [20, 29]. It can be concluded that obliqueness of the propagation has a strong effect over propagation with subsonic speed as compared to supersonic speed.

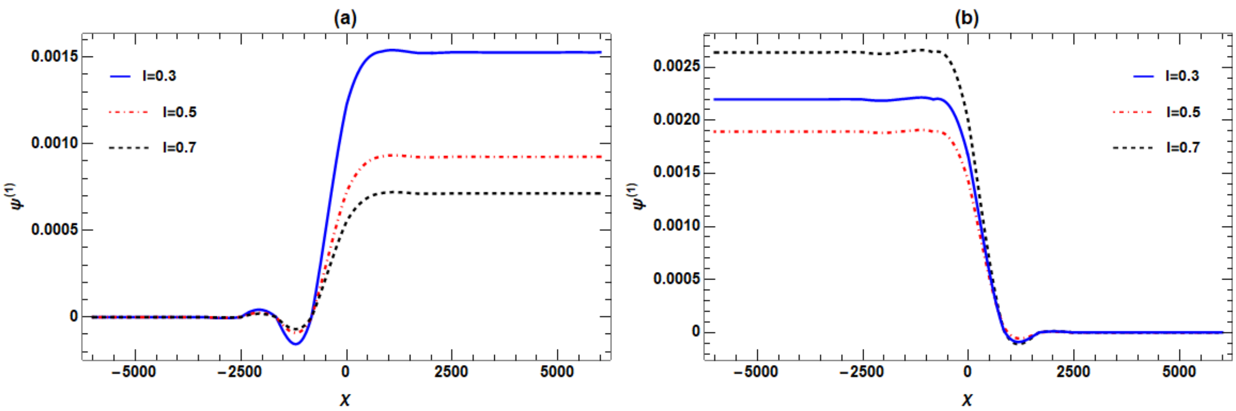

Figure 4. Showing the profile $\psi^{(1)}$ of IAShWs that represented by Eq. (20) against χ with combination of different normalized density values $\mu_{m,}$ μ_e and μ_p for $(a)\lambda<1$ and $(b)\lambda>1$, while the values of other parameter is considered as $\delta_+=0.5,$ $\delta_-=0.5,$ $\Omega_+=0.6, \Omega_+=0.16,$ $l=0.3,$ $p_{+\|}=0.5, p_{+\perp}=0.2, p_{-\|}=0.3$ & $p_{-\perp}=0.2$

Fig. 5 shows the graphical presentation of IAShWs profile of normalized potential function $\psi^{(1)}$ against χ with different combination of external magnetic field provided to positive (Ω_+) and negative (Ω_-) ions for both (a) subsonic and (b) supersonic modes of normalized phase velocity. Fig 5(a) & 5(b) clearly show that as the strength of the external magnetic field increases, both the amplitude and steepness of the shock wave also rise. Moreover, the sharpness of the shock wave becomes increasingly noticeable. It is clear from both the figures that as the cyclotron frequency of positive ion's increases significantly compared to electron's cyclotron frequency, and as we know, higher magnetic field is required to magnetize the positive ions than compared to electrons, all the low energy electrons can escape such high magnetic field there causing enhancement in the energy of the wave and thus amplitude of the wave increases significantly. This research explores how the strength of the magnetic field affects the properties of the IAShWs profile by examining the dispersion coefficient in relation to the normalized cyclotron frequency [35,38].

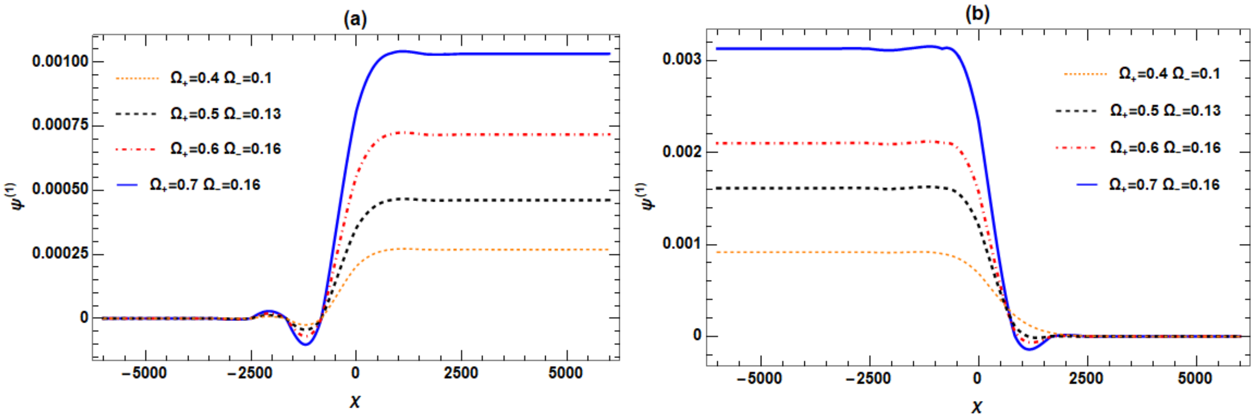

Figure 5. The profile $\psi^{(1)}$ of IAShWs with respect to χ for a combination of different normalized density values $\mu_{m,}$ μ_e and μ_p for $(a)\lambda<1$ and $(b)\lambda>1$, the values of other parameters are considered as $\delta_+=0.5$, $\delta_-=0.5$, $\Omega_+=0.6, \Omega_+=0.16$, $l=0.3$, $p_{+\parallel}=0.5, p_{+\perp}=0.2, p_{-\parallel}=0.3$ & $p_{-\perp}=0.2$

Fig. 6 shows the graphical presentation of IAShWs profile of normalized potential function $\psi^{(1)}$ against χ with different kinematic and bulk viscosity of the pair of ions (as dissipative parameter δ_+ and δ_-) for both (a) subsonic and (b) supersonic phase speed. From Fig. 6(a) (Subsonic phase speed), it is clearly seen that viscosity of positive ion reduces the IAShWs profile, while negative ion viscosity enhances the profile. It might be because, as the negative ion viscosity increases (i.e. overall reduction in the velocity of the negative ions), the more and more low energy electrons will be captured in the surface of the heavy negative ions, and eventually, the left behind electrons will be of only high energy, and this enhances the amplitude of the wave. On the other hand, from Fig. 6(b) (Supersonic phase speed), it is seen that the profile of IAShWs profile enhances with positive ion viscosity which is reduces for negative ion viscosity [34,36,37].

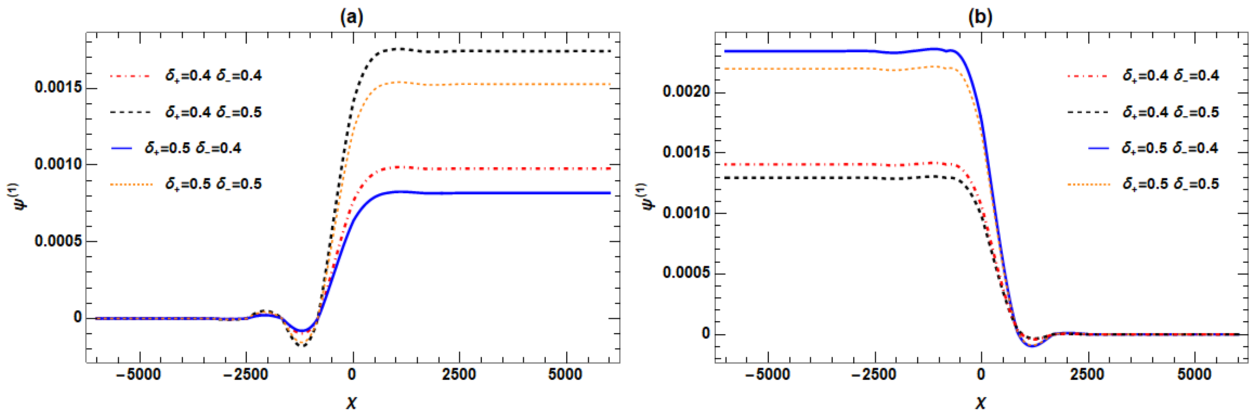

Figure 6. Showing the profile $\psi^{(1)}$ of IAShWs that represented by Eq. (20) against χ with combination of different normalized density values $\mu_{m,}$ μ_e and μ_p for $(a)\lambda<1$ and $(b)\lambda>1$, while the values of other parameter is considered as $\delta_+=0.5$, $\delta_-=0.5$, $\Omega_+=0.6$, $\Omega_+=0.16$, $l=0.3$, $p_{+\parallel}=0.5, p_{+\perp}=0.2, p_{-\parallel}=0.3$ & $p_{-\perp}=0.2$.

To know the effect of pressure anisotropy on the characteristics of IAShWs, we depict the variation of $\psi^{(1)}$ w.r.t χ for different values of $p_{+\parallel}, p_{+\perp}, p_{-\parallel}$ and $p_{+\perp}=0.2$ (for fixed values of other parameter). From Fig.7(a) i.e. when the normalized phase speed is in subsonic mode, we have observed that when the thermal pressure of positive ions increases in both parallel and perpendicular direction $\left(p_{+\parallel}\,\&\,p_{+\perp}\right)$ increases the amplitude and steepness of the shock profiles whereas the increase in thermal pressure of negative ion in perpendicular direction decreases the amplitude and steepness of the wave. However, from Fig.7(b) i.e. when the normalized phase speed is in supersonic mode, it is noticed that increasing the parallel thermal pressure of positive ion $\left(p_{+\parallel}\right)$ enhances the amplitude as well as steepness of shock waves profile, but increasing the parallel thermal pressure of negative ion $\left(p_{-\parallel}\right)$ reduces the amplitude of the shock structure [34,38].

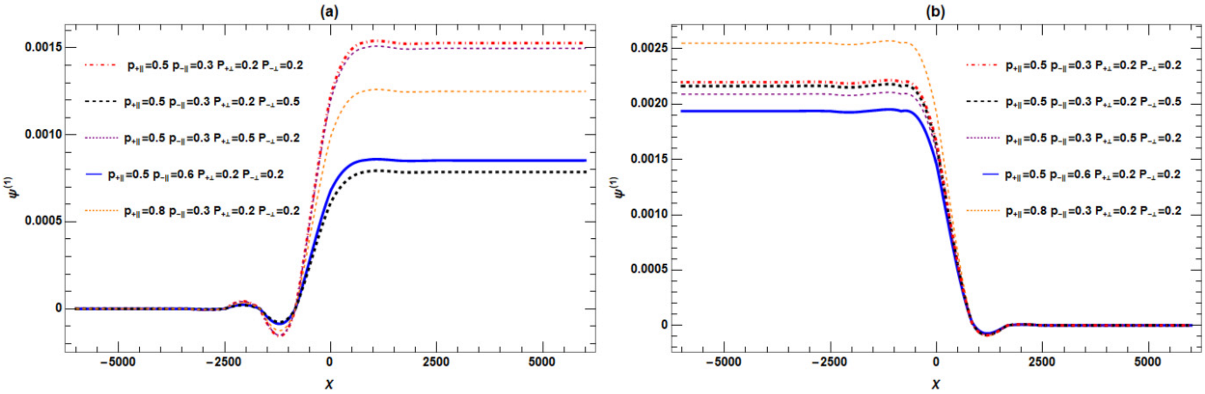

Figure 7. Showing the profile $\psi^{(1)}$ of IAShWs that represented by Eq. (20) against χ with combination of different normalized density values $\mu_{m,}$ μ_e and μ_p for $(a)\lambda<1$ and $(b)\lambda>1$, while the values of other parameter is considered as $\delta_+=0.5,$ $\delta_-=0.5,$ $\Omega_+=0.6, \Omega_+=0.16$ & $l=0.3$

Fig.8 shows the graphical presentation of IAShWs profile of normalized potential function $\psi^{(1)}$ against χ with different combination of density ratio of negative ion $\left(\mu_m\right)$, electron $\left(\mu_e\right)$ and positron $\left(\mu_p\right)$ w.r.t positive ion for both (a) subsonic and (b) supersonic modes of normalized phase velocity. It can be noticed from both figures that as we increases μ_e from 0.7 to 0.8 and μ_p from 0.1 to 0.2 by keeping μ_m as 0.4 (red dot dashed & black dashed) the amplitude and steepness of IAShWs increases when the phase speed is in subsonic mode, which on the other hand reduces for supersonic mode. In similar manner we see for other curves of Fig. 8(a) & 8(b) as we increasing the values of any two parameter μ_m, μ_p and μ_e by keeping third one same value, it is observed that amplitude and steepness of the shock structure declines. An oscillating shock wave pattern is linked to the potential profile when the electron density achieves a critical threshold. When the electron count is insufficient to shield against the potential, positive ions work to increase the electron pressure, facilitating the formation of an oscillating structure. However, the potential of this structure remains unshielded. As a result, a reduction in electron density within the plasma leads to a decrease in both the amplitude and steepness of the wave. This relationship highlights the delicate balance between electron density and the stability of oscillatory structures, illustrating the dynamic interplay between charged particles in the plasma environment. [32,39]

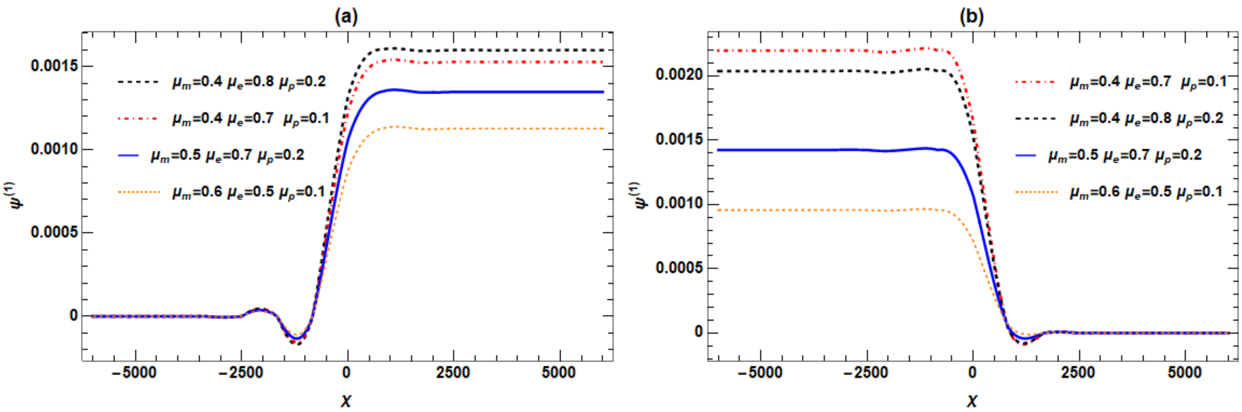

Figure 8. Showing the profile $\psi^{(1)}$ of IAShWs that represented by Eq. (20) against χ with combination of different normalized density values $\mu_{m,}$ μ_e and μ_p for $(a)\lambda<1$ and $(b)\lambda>1$, while the values of other parameter is considered as $\delta_+=0.5,$ $\delta_-=0.5,$ $\Omega_+=0.6, \Omega_+=0.16,$ $l=0.3,$ $p_{+\parallel}=0.5, p_{+\perp}=0.2, p_{-\parallel}=0.3$ & $p_{-\perp}=0.2$.

5. PHASE PORTRAIT ANALYSIS

The results of travelling wave solutions of a differential equation (DE) can also be analyzed through phase portrait analysis. For this phase portrait analysis, we convert the second order DE into two first order ordinary DEs in a system as follows [8,35,40]:

$$\left.\begin{aligned}\frac{d\psi^{(1)}}{d\chi}&=y\\ \frac{dy}{d\chi}&=\frac{U}{G}\psi^{(1)}-\frac{Bl}{2G}\left(\psi^{(1)}\right)^{2}+\frac{H}{G}y\end{aligned}\right\} \tag{21}$$

From this planner dynamical system (PDS)(Eq.21) the corresponding Jacobian matrix is

$$\mathrm{J}=\begin{pmatrix}0 & 1\\ \dfrac{U}{G}-\dfrac{Bl}{2G}\psi^{(1)} & \dfrac{H}{G}\end{pmatrix} \tag{22}$$

The system (21) has two equilibrium points which are stated as $\left(\psi_i^{(1)},0\right)$ for $i=0$ and 1. The trace$\left(T_i\right)$ and determinant$\left(\Delta_i\right)$ of the above Jacobian matrix decides the stability of the system at these equilibrium points. Let the elements of the Jacobian matrix be $\Delta_i=\det\left(\mathrm{J}\left(\psi_i^{(1)},0\right)\right)$ and $T_i=trace\left(\mathrm{J}\left(\psi_i^{(1)},0\right)\right)$. Then using the concept of dynamical systems [31,37-40], the equilibrium points $\left(\psi_i^{(1)},0\right)$ is a saddle point for $\Delta_i<0$, a center point for $\Delta_i>0, T_i=0$, a stable spiral for $T_i<0$ and $T_i^2-4\Delta_i<0$, an unstable spiral for $T_i>0$ and $T_i^2-4\Delta<0$, and node for $T_i^2-4\Delta>0$.

Figure 9(a) subsonic and 9(b) supersonic shown that the PDS (22) has two equilibrium configurations at $C_0(0,0)$ and $C_1\left((2U/Bl)^2,0\right)$. To examine the stability of the system (22), we use the values of some typical parameter as $\beta_e=0.2$, $\beta_p=0.2$, $\delta_+=0.1$, $\delta_-=0.1$, $\mu_m=0.4$, $\mu_p=0.7$ and $U>0$, the critical point C_1 has $\Delta<0$, thus this is a saddle point. Again, the critical C_0 satisfies $T_1=0$ and $\Delta_i>0$ .Thus the critical point $C_0(0,0)$ is a center. From both the figure we conclude that there are trajectories from $(-0.005,0)$ and $(0.005,0)$ connecting two saddle points. The existence of these heteroclinic orbit corresponds to occurrence of shock wave profile.

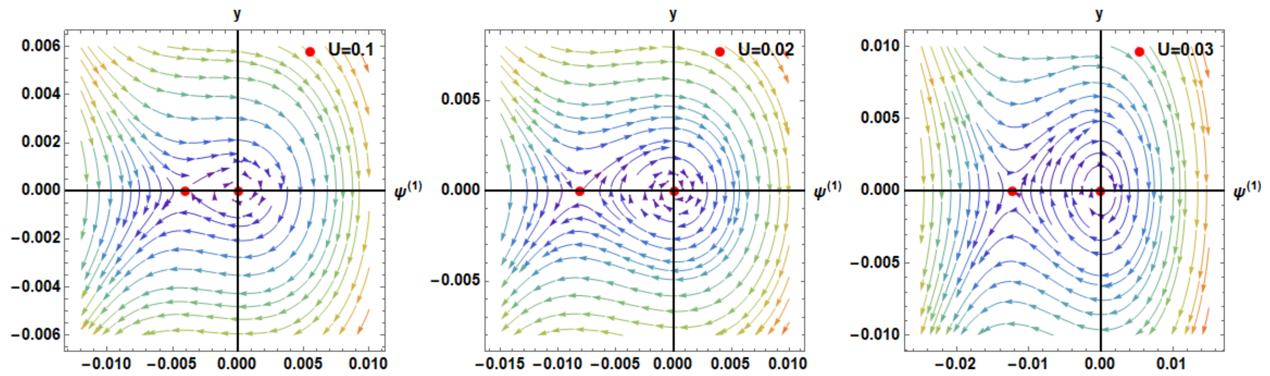

Figure 9(a). Phase portrait of the system (Eq. (21)) for different values of travelling wave speed U while $\delta_+=0.5$, $\delta_-=0.5$, $\Omega_+=0.4,\Omega_+=0.1$, $l=0.3$, $p_{+\parallel}=0.5, p_{+\perp}=0.2, p_{-\parallel}=0.3$ & $p_{-\perp}=0.2$ for the lower Mach number

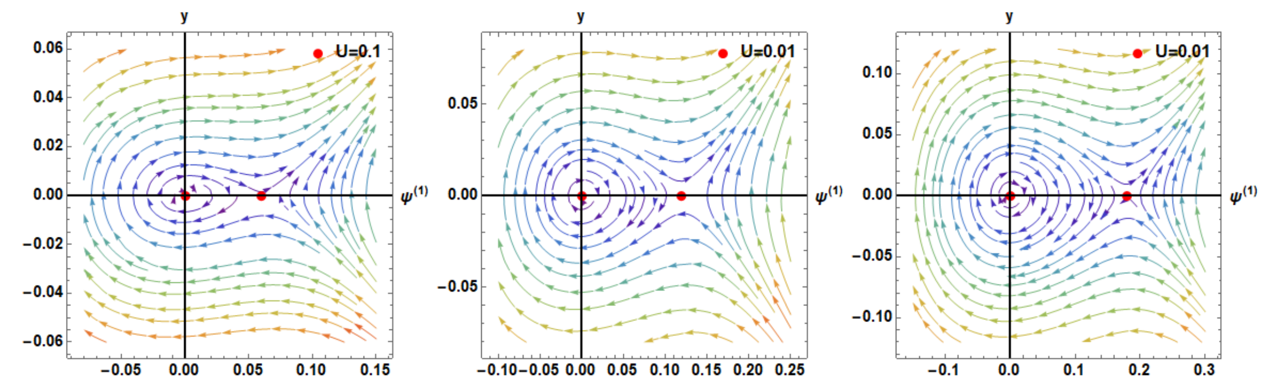

Figure 9(b). Phase portrait of the system (Eq. (21)) for different values of travelling wave speed U while $\delta_+=0.5$, $\delta_-=0.5$, $\Omega_+=0.4,\Omega_+=0.1$, $l=0.3$, $p_{+\parallel}=0.5$, $p_{+\perp}=0.2$, $p_{-\parallel}=0.3$ & $p_{-\perp}=0.2$ for the lower Mach number

6. CONCLUSION

In conclusion, we investigate the effect of trapping of electron & positron and anisotropic pressure as well as viscosity on IAShWs in degenerate plasma. With the help of method of reductive perturbation, we derived the well-known ZKB equation. The effect of density ratio of negative ion, electron and positron w.r.t positive ions, magnetic field, anisotropic pressure & viscosity for both positive and negative ions are investigated briefly. Next, we will convert our evolutionary equation into a two-dimensional dynamical system and conduct a phase-plane analysis. The results of our research could have practical applications in several situations involving space observation and astrophysics, particularly when dealing with trapped electrons and pressure anisotropy.

Declarations
Availability of data and materials: Not applicable. No new data were created or analyzed in this study.
Competing interests: The authors declare that they have no competing interests.
Authors' contributions: BP contributed in Plotting Graphs and writing the manuscript, AND contributed in forming model, methodology and supervised the manuscript. MKD contributed in editing of the manuscript.

ORCID
Balaram Pradhan, https://orcid.org/0009-0005-8093-8035; **Apul Narayan Dev,** https://orcid.org/0000-0002-4478-5204
Manoj Kumar Deka, https://orcid.org/0000-0001-8011-9930

REFERENCE

[1] A.A. Mamun, and P.K. Shukla, "Solitary waves in an ultrarelativistic degenerate dense plasma," Phys. Plasmas, **17**, 104504 (2010). https://doi.org/10.1063/1.3491433
[2] W.M. Moslem, "Self-similar expansion of white dwarfs. Astrophys," Space Sci. **342**, 351-355 (2012). https://doi.org/10.1007/s10509-012-1185-4
[3] N. Roy, S. Tasnim, and A.A. Mamun, "Solitary waves and double layers in an ultra-relativistic degenerate dusty electron-positron-ion plasma," Phys. Plasmas, **19**, 033705 (2012). https://doi.org/10.1063/1.3688877
[4] I. Zeba, W.M. Moslem, and P.K. Shukla, "Ion solitary pulses in warm plasmas with ultrarelativistic degenerate electrons and positrons," Astrophys. J. **750**, 72 (2012). https://doi.org/10.1088/0004-637X/750/1/72
[5] S.A. Shan, A. Ur-Rehman, and A. Mushtaq, "Ion-acoustic solitary waves in a positron beam plasma with electron trapping and nonextensivity effects," Phys. Plasmas, **24**, 032104 (2017). https://doi.org/10.1063/1.4978294
[6] A.U. Rahman, S. Ali, A. Mushtaq, and A. Qamar, "Nonlinear ion acoustic excitations in relativistic degenerate, astrophysical electron–positron–ion plasmas," J. Plasma Phys. **79**, 817-823 (2013). https://doi.org/10.1017/S0022377813000524
[7] B. Hosen, M.G. Shah, R.M. Hossen, and A.A. Mamun, "Ion-acoustic solitary waves and double layers in a magnetized degenerate quantum plasma," IEEE Trans. Plasma Sci. **45**, 3316-3327 (2017). https://doi.org/10.1109/TPS.2017.2766167
[8] A. Abdikian, A. Saha, and S. Alimirzaei, "Bifurcation analysis of ion-acoustic waves in an adiabatic trapped electron and warm ion plasma." J. Taibah Univ. Sci. **14**, 1051-1058 (2020). https://doi.org/10.1080/16583655.2020.1798062
[9] M.K. Islam, S. Biswas, N.A. Chowdhury, A. Mannan, M. Salahuddin, and A.A. Mamun, "Obliquely propagating ion-acoustic shock waves in a degenerate quantum plasma," Contrib. Plasma Phys. **62**, 202100073 (2022). https://doi.org/10.1002/ctpp.202100073
[10] M.M. Haider, and A.A. Mamun, "Ion-acoustic solitary waves and their multi-dimensional instability in a magnetized degenerate plasma," Phys. Plasmas. **19**, 102105 (2012). https://doi.org/10.1063/1.4757218
[11] A. Abdikian, and B. Ghanbari, "On a modified Korteweg–de Vries equation for electrostatic structures in relativistic degenerate electron–positron plasma," Results Phys. **48**, 106399 (2023). https://doi.org/10.1016/j.rinp.2023.106399
[12] M. Adnan, G. Williams, A. Qamar, S. Mahmood, and I. Kourakis, "Pressure anisotropy effects on nonlinear electrostatic excitations in magnetized electron-positron-ion plasmas," Eur. Phys. J. D, **68**, 1-15 (2014). https://doi.org/10.1140/epjd/e2014-50384-y
[13] M.K. Deka, B. Pradhan, A.N. Dev, D. Mahanta, J. Manafian, and K.H. Mahmoud, "Shock Waves in Ion-Beam-Depleted Spin-Polarized Quantum Plasma with Ionic Pressure Anisotropy," Plasma, **8**, 3 (2025). https://doi.org/10.3390/plasma8010003
[14] M. Ahmad, M. Adnan, and A. Qamar, "Magnetosonic shock waves in degenerate electron–positron–ion plasma with separated spin densities," Phys. Fluids, **36**, 087115 (2024). https://doi.org/10.1063/5.0216452
[15] R. Jahangir, and S. Ali, "Nonlinear ion-acoustic waves in degenerate plasma with landau quantized trapped electrons," Front. Phys. **9**, 622820 (2021). https://doi.org/10.3389/fphy.2021.622820
[16] H. Schamel, and B. Sarbeswar, "Analytical double layers," Phys. Fluids, **26**, 190-193 (1983). https://doi.org/10.1063/1.864006
[17] H. Schamel, "Weak double layers: Existence, stability, evidence," Z. fur Naturforsch. - J. Phys. Sci. **38**, 1170-1183 (1983). https://doi.org/10.1515/zna-1983-1102
[18] H. Schamel, and V.I. Maslov, "Adiabatic growth of electron holes in current-carrying plasmas," Phys. Scr. **50**, 42 (1994). https://doi.org/10.1088/0031-8949/1994/T50/006
[19] V. Maslov, and H. Schamel, "Growing electron holes in drifting plasmas," Phys. Lett. A, **178**, 171-174 (1993). https://doi.org/10.1016/0375-9601(93)90746-M
[20] R. Kaur, and N.S. Saini, "Ion acoustic shocks in a weakly relativistic ion-beam degenerate magnetoplasma," Galaxies, **9**, 64 (2021). https://doi.org/10.3390/galaxies9030064
[21] M.J. Iqbal, W. Masood, H.A. Shah, and N.L. Tsintsadze, "Nonlinear density excitations in electron-positron-ion plasmas with trapping in a quantizing magnetic field," Phys. Plasmas, **24**, 014503 (2017). https://doi.org/10.1063/1.4973830
[22] M.A. El-Borie, M. Abd-Elzaher, and A. Atteya, "Obliquely propagating ion-acoustic solitary and shock waves in magnetized quantum degenerate multi-ions plasma in the presence of trapped electrons," Chin. J. Phys. **63**, 258-270 (2020). https://doi.org/10.1016/j.cjph.2019.10.004

[23] H.A. Shah, M.N.S. Qureshi, and N. Tsintsadze, "Effect of trapping in degenerate quantum plasmas," Phys. Plasmas, **17**, 032312 (2010). https://doi.org/10.1063/1.3368831
[24] S.Y. El-Monier, and A. Atteya, "Dynamics of ion-acoustic waves in nonrelativistic magnetized multi-ion quantum plasma: the role of trapped electrons," Waves Random Complex Media, **32**, 299-317 (2022). https://doi.org/10.1080/17455030.2020.1772522
[25] T. Yeashna, R.K. Shikha, N.A. Chowdhury, A. Mannan, S. Sultana, and A. Mamun, "Ion-acoustic shock waves in magnetized pair-ion plasma," Eur. Phys. J. D, **75**, 1-7 (2021). https://doi.org/10.1140/epjd/s10053-021-00139-y
[26] N.A. Zedan, A. Atteya, W.F. El-Taibany, and S.K. El-Labany, "Stability of ion-acoustic solitons in a multi-ion degenerate plasma with the effects of trapping and polarization under the influence of quantizing magnetic field," Waves Random Complex Media, **32**, 728-742 (2022). https://doi.org/10.1080/17455030.2020.1798560
[27] P. Halder, K.N. Mukta, and A.A. Mamun, "Nonlinear propagation of dust-ion-acoustic shock waves in a degenerate multi-species plasma," Int. J. Cosmol. Astron. Astrophys. **1**, 81-87 (2019). http://dx.doi.org/10.18689/ijcaa-1000119
[28] S. Hussain, H. Ur-Rehman, and S. Mahmood, " The effect of magnetic field quantization on the propagation of shock waves in quantum plasmas," Phys. Plasmas. 26, 052105 (2019). https://doi.org/10.1063/1.5090181
[29] M. Asaduzzaman, M.A.A. Mamun, and A.A. Mamun, "Obliquely Propagating Self-Gravitational Shock Waves in Non-Relativistic Degenerate Quantum Plasmas," J. Eng. Sci. Technol. Rev. **15**(1), 21-29 (2024). https://doi.org/10.3329/jes.v15i1.76030
[30] M.K. Deka, and A.N. Dev, "Wave propagation with degenerate electron–positron in magnetically quantised ion beam plasma," Pramana, **95**, 65 (2021). https://doi.org/10.1007/s12043-021-02081-5
[31] M. Irfan, S. Ali, and A.M. Mirza, "Solitary waves in a degenerate relativistic plasma with ionic pressure anisotropy and electron trapping effects," Phys. Plasmas. **24**, 052108 (2017). https://doi.org/10.1063/1.4981932
[32] S. Jahan, T.S. Roy, B.E. Sharmin, N.A. Chowdhury, A. Mannan, and A.A. Mamun, "Magnetized ion-acoustic shock waves in degenerate quantum plasma," arXiv preprint arXiv 2103, 15863 (2021). https://doi.org/10.48550/arXiv.2103.15863
[33] A. Ur-Rahman, I. Kourakis, and A. Qamar, "Electrostatic solitary waves in relativistic degenerate electron–positron–ion plasma," IEEE Trans. Plasma Sci. **43**, 974-984 (2015). https://doi.org/10.1109/TPS.2015.2404298
[34] M.K. Deka, D. Mahanta, A.N. Dev, J. Sarma, S.K. Mishra, E. Saikia, "Features of shock wave in a quantized magneto plasma under the influence of ionic pressure anisotropy and anisotropic viscosity," AIP Conf. Proc. **2819**, 070005 (2023). https://doi.org/10.1063/5.0137746
[35] I. Alazman, B.S.T. Alkahtani, M. Ur-Rahman, and M.N. Mishra, "Nonlinear complex dynamical analysis and solitary waves for the (3+1)-D nonlinear extended Quantum Zakharov–Kuznetsov equation," Results Phys. **58**, 107432 (2024). https://doi.org/10.1016/j.rinp.2024.107432
[36] W. Albalawi, M.M. Hammad, M. Khalid, A. Kabir, C.G. Tiofack, and S.A. El-Tantawy, "On the shock wave structures in anisotropy magnetoplasmas," AIP Advances, **13**, 105309 (2023). https://doi.org/10.1063/5.0173000
[37] B. Boro, A.N. Dev, B.K. Saikia, and N.C. Adhikary, "Nonlinear dust ion acoustic shock wave structures in solar F corona region," Phys. Plasmas, **27**, 122901 (2020). https://doi.org/10.1063/5.0023283
[38] B. Pradhan, B. Boro, A.N. Dev, J. Manafian, and N.A. Alkader, "Effect of ion anisotropy pressure in viscous plasmas: evolution of shock wave," Nonlinear Dyn. **112**, 17403-17416 (2024). https://doi.org/10.1007/s11071-024-09994-x
[39] S. Jahan, B.E. Sharmin, N.A. Chowdhury, A. Mannan, T.S. Roy, and A.A. Mamun, "Electrostatic ion-acoustic shock waves in a magnetized degenerate quantum plasma," Plasma, **4**, 426-434 (2021). https://doi.org/10.3390/plasma4030031
[40] T. Sarkar, S. Roy, S. Raut, and P.C. Mali, "Studies on the dust acoustic shock, solitary, and periodic waves in an unmagnetized viscous dusty plasma with two-temperature ions," Braz. J. Phys. **53**, 12 (2023). https://doi.org/10.1007/s13538-022-01221-5
[41] Z. Iqbal, H.A. Shah, M.N.S. Qureshi, W. Masood, and A. Fayyaz, "Nonlinear dynamical analysis of drift ion acoustic shock waves in Electron-Positron-Ion plasma with adiabatic trapping," Results Phys. **41**, 105948 (2022). https://doi.org/10.1016/j.rinp.2022.105948
[42] A. Atteya, M.A. El-Borie, G.D. Roston, A.A.S. El-Helbawy, P.K. Prasad, and A. Saha, "Ion-acoustic stable oscillations, solitary, periodic and shock waves in a quantum magnetized electron–positron–ion plasma," Z. fur Naturforsch. - J. Phys. Sci. **76**, 757-768 (2021). https://doi.org/10.1515/zna-2021-0060
[43] S.N. Chow, and J.K. Hale, *Methods of bifurcation theory*, (Springer Science & Business Media, 2012).
[44] J. Guckenheimer, and P. Holmes, *Nonlinear oscillations, dynamical systems, and bifurcations of vector fields*, (Springer Science & Business Media, 2013).

ПОШИРЕННЯ ХВИЛЬ В АНІЗОТРОПНІЙ МАГНІТНО-КВАНТОВАНІЙ ІОННІЙ ПЛАЗМІ З ЗАХОПЛЕНИМИ ЕЛЕКТРОНАМИ ТА ПОЗИТРОНАМИ

Баларам Прадхан[a], Апул Нарайан Дев[b], Манодж Кумар Дека[c]
[a]*Центр науки про дані, Сікша «О» Анусандхан (вважається університетом), Хандагірі, Бхубнешвар 751030, Одіша, Індія*
[b]*Кафедра математики, Сікша «О» Анусандхан (вважається університетом), Хандагірі, Бхубнешвар 751030, Одіша, Індія*
[c]*Кафедра радіографії та технологій візуалізації, Університет медичних наук імені Шріманти Шанкарадеви, Гувахаті 781032, Індія*

Це дослідження розглядає вплив магнітно квантованих вироджених захоплених електронів та позитронів на іонно-акустичні ударні хвилі (ІАУХ) малої амплітуди в парній іонній плазмі за допомогою рівняння Захарова-Кузнецова-Бюргера (ZKB). Воно зосереджується на тому, як такі фактори, як магнітне квантування, вироджена температура, нормалізовані негативні іони, електрони, позитрони, анізотропний тиск та інші відповідні фізичні параметри з астрофізичного плазмового середовища, впливають на поширення ІАУХ, особливо в нелінійному режимі. Це дослідження досліджує, що існують два різних режими поширення хвиль — дозвуковий та надзвуковий, які демонструють мало відмінних характеристик у різних фізичних плазмових середовищах астрофізичного походження. Результати можуть допомогти в розумінні нелінійної динаміки та характеристик поширення хвиль у надщільній плазмі, що зустрічається в білих карликах та нейтронних зірках, де вплив захоплених електронів та позитронів, а також анізотропія іонного тиску, є значним, що ще потребує детального вивчення.
Ключові слова: *намагнічена плазма; дозвуковий та надзвуковий режими; метод відновних збурень (RPT); вироджені захоплені електрони та позитрони; рівняння ZKB; аналіз фазової площини*